

Antimicrobial Photodynamic Activity of Gallium-Substituted Haemoglobin on Silver Nanoparticles: Electronic Supplementary Information

Preparation and characterization of GaHb (Fig. S1, S2)	S-1
Preparation and characterization of GaHb–AgNPs (Fig. S3–S6, Table S1).....	S-3
Preparation and characterization of GaHb–AuNPs (Fig. S7)	S-7
Cytotoxicity studies of GaHb–AgNPs using HaCaT and J774 cells (Fig. S8, S9).....	S-7
Additional TEM images of <i>S. aureus</i> labeled with 10-nm GaHb–AgNPs (Fig. S10).	S-9
Studies involving MRSA persister cells and intracellular MRSA.....	S-10
Light sources for antimicrobial photodynamic inactivation	S-10

Preparation and characterization of GaHb

Commercially available haemoglobin (Hb, Sigma) was treated with mild acid to remove its hemin cofactor by extraction to obtain apoHb, following a literature procedure.²⁶ 53 mg of Hb was dissolved at 0 °C in 5 mL of chilled water; the solution was adjusted to pH 2 by dropwise addition of 3 M HCl, then treated with 10 mL of cold ethyl methyl ketone while stirring. The solution was maintained at 0 °C throughout this process and allowed to stand for 2–3 minutes until a clear separation of layers was observed. The organic layer containing free haeme was removed, and the aqueous layer was washed extensively with ethyl methyl ketone (4 × 10 mL) for further removal of heme. The apoHb solution was transferred to dialysis tubing (12 kDa MWCO) and dialyzed first against deionized water, then PBS (pH 7.4), then again with pure water. Removal of hemin from Hb was confirmed by the disappearance of the Soret band (λ_{\max} ~400 nm) from the absorbance spectrum. apoHb could be lyophilized and stored as a solid at 4 °C for future use.

To prepare GaHb, a solution of GaPpIX (4 equiv) in 0.01 M sodium hydroxide (0.6 mg in 200 μ L) was added to a chilled solution of apoHb (1 equiv) in 0.1 M PBS at pH 6.5 (15 mg in 10 mL), and slowly stirred for 3 h at 0 °C to yield GaHb. The reaction mixture was subjected to centrifugation at 4000 rpm (2700 g) for 10 min to remove precipitated proteins, then passed through a Sephadex–G25 column using 0.01 M PBS at pH 6.3 to remove unbound GaPpIX. GaHb solution was dialyzed against PBS and deionized water, and could be lyophilized and stored as a pink solid. GaHb formation was characterized by the reappearance of a Soret band (λ_{\max} 416 nm; **Figure 2a**).

SDS-PAGE of Hb, apoHb, and GaHb produced nearly identical band patterns indicative of $\alpha\beta$ dimers (32 kDa) and $\alpha_2\beta_2$ tetramers (64 kDa); a minor band below 50 kDa could also be detected, possibly corresponding to a trimer (Figure S1). A titration of GaPpIX to apoHb indicated a linear increase in the absorbance peak intensity at 416 nm (Figure S2). Interestingly, Job plot analysis revealed a linear increase in absorbance at 416 nm for up to 6 mole equivalents of GaPpIX, which suggests that additional protoporphyrins can be incorporated between apoHb subunits.

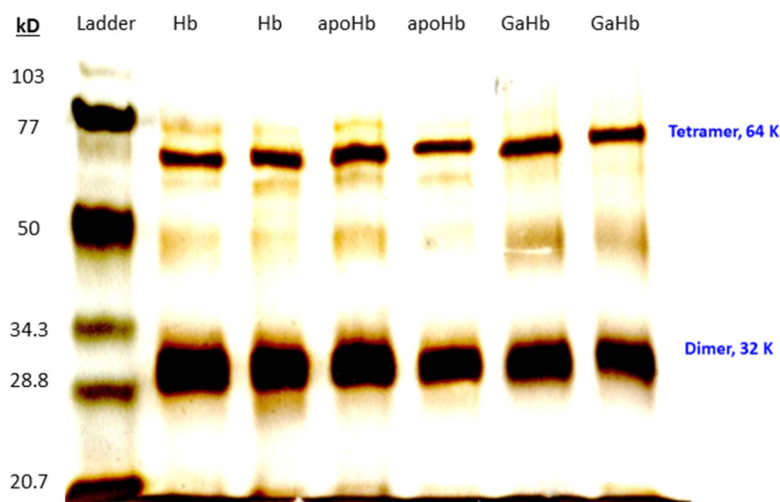


Figure S1. SDS-PAGE analysis of Hb, apoHb, and GaHb.

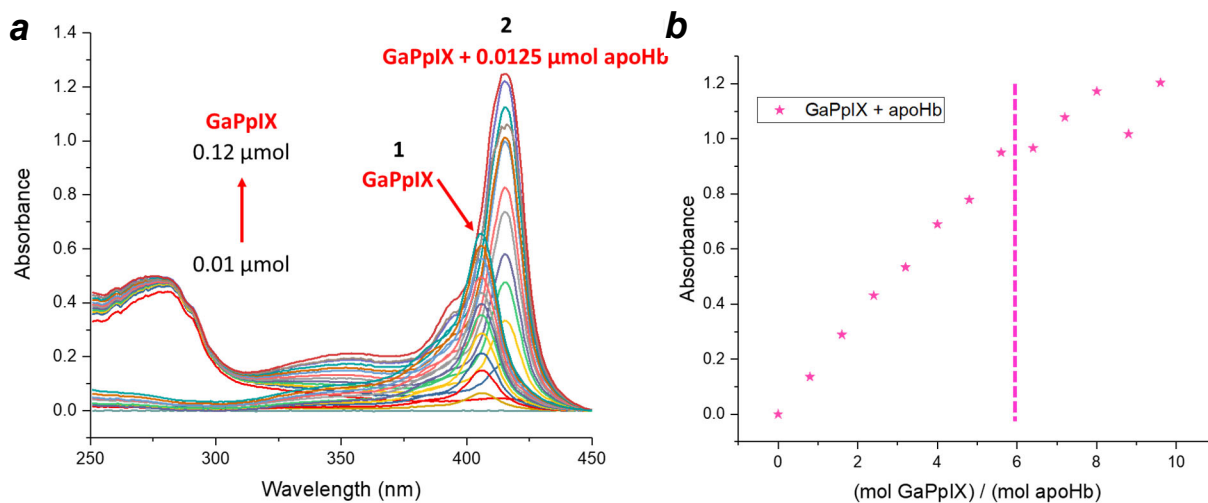


Figure S2. (a) UV-vis spectra of titration of GaPpIX (0.01–0.12 μmol) added to (1) phosphate buffer saline solution (PBS) and (2) 0.0125 μmol apoHb. (b) Job plot of GaHb formation as a function of GaPpIX mole equivalents, using 0.0125 μmol apoHb. A linear increase in absorbance at 416 nm was observed for up to 6 GaPpIX equivalents.

The binding constant between GaPpIX and apoHb subunits was measured in triplicate at 25 °C by fluorescence polarization using a Spark 10M multimode microplate reader (Tecan; $\lambda_{\text{ex/em}}$ 405/585 nm). Various concentrations of apoHb (10–1000 nM; $\alpha\beta$ form) were mixed with 100 nM GaPpIX in a black 96-well plate (Corning Costar) and incubated at 4 °C for 4 h on a shaker protected from light. An experimental K_d ($1/K_d$) value of 24 nM was obtained by measuring relative changes in fluorescence intensity (ΔI) as a function of apoHb dimer concentration, and fitting the data to the Langmuir–Freundlich isotherm model (OriginPro); multiplying the experimental value yields K_d per binding site (48 nM), assuming the absence of allosteric effects (**Figure 2c**).

Preparation and characterization of GaHb–AgNPs

Ag nanoparticles were obtained as 20 $\mu\text{g/mL}$ solutions in sodium citrate buffer (pH 7.7) from a commercial source (NanoComposix). A 10-mL solution of 10- or 40-nm citrate-stabilized AgNPs was centrifuged at 900 g for 5 min, then decanted and mixed with 200 μL of GaHb in PBS (1 mg/mL, pH 7.4), near the isoelectric point of bovine Hb (pH 7.1). The mixture was slowly stirred overnight at 4 °C, then transferred to a centrifugal filter tube (Centricon, 100-kDa MWCO) and subjected to 2700 g for 5 min, followed by dilution of the residual AgNP suspension in 15 mM borate buffer (pH 8.5). In the case of 40-nm AgNPs, the mixture was transferred to a standard centrifuge tube and subjected to 3300 g for 20 min, followed by disposal of the supernatant and redispersion of the AgNP retentate in 15 mM borate buffer. Each procedure was performed three times prior to GaHb–AgNP characterization.

Both 10- and 40-nm GaHb-coated AgNPs exhibited a slight redshift in plasmon resonance compared to uncoated NPs; a shoulder between 450–500 nm indicated the presence of some aggregates (**Figure S3a,b**), however TEM analysis indicates the majority of GaHb–AgNPs to be well dispersed (**Figure S3c,d**). The absorbance maximum for 10-nm GaHb–AgNPs is 396 nm (3-nm redshift vs. 10-nm AgNP), and 419 nm for 40-nm GaHb–AgNPs (4-nm redshift vs. 40-nm AgNP).

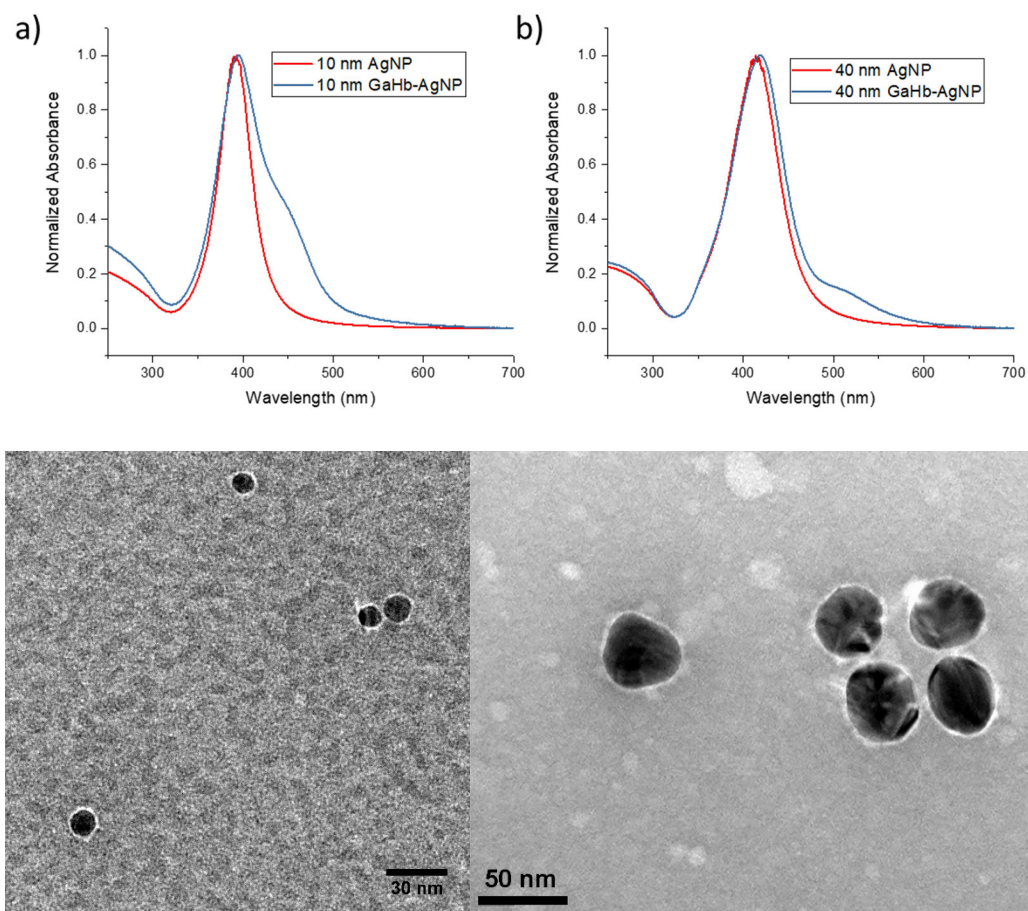


Figure S3. (a,b) Absorption spectra of GaHb–AgNP assemblies with 10- and 40-nm cores. (c,d) Negative-stain TEM images of GaHb–AgNPs (Tecnai T20, 80–100 kV), with 10- and 40-nm cores, supporting the presence of dense protein coats around the AgNP cores.

To determine the amount of GaHb adsorbed onto AgNPs, we used a Bradford assay with Coomassie Blue (λ_{\max} 595 nm) with a standard curve using known quantities of GaHb (**Figure S4**). GaHb-coated AgNPs at three different concentrations were centrifuged and redispersed in deionized water, then digested using NaCN and subjected to analysis along with a negative control. For 10-nm GaHb–AgNPs, this yielded a weight ratio of 1 μg GaHb per 7.4 μg Ag, or nearly 7 GaHb per 10-nm AgNP based on the density of Ag (10.5 g/cm³), corresponding to a monolayer of protein. For 40-nm GaHb–AgNPs, a weight ratio of 1 μg GaHb per 4.8 μg Ag was obtained, corresponding to 688 GaHb per 40-nm AgNP, corresponding to a multilayer of protein. Negative-stain TEM analysis of GaHb–AgNPs confirmed dense hydrophobic coatings around the AgNP cores (**Figure S3c,d**).

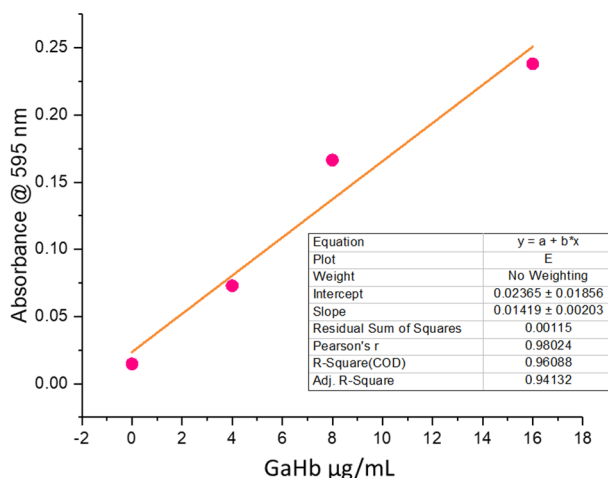


Figure S4. (a) Calibration curve from Bradford assay, using GaHb.

Hydrodynamic sizes (d_h) and zeta potentials of the GaHb–AgNPs were determined by DLS in 15 mM borate buffer at pH 8.5 (**Table S1**). The 10-nm AgNP cores (as described by the supplier) were found to have a mean d_h of 14 nm. For 10-nm GaHb-coated AgNPs, the mean d_h increased to 17 nm (**Figure S5a,b**), and the zeta potential shifted by +15 mV relative to citrate-stabilized AgNPs (**Figure S6a,b**). For the 40-nm GaHb–AgNPs, the mean hydrodynamic size reduced slightly from 36 nm to 34 nm (**Figure S5c,d**), and the zeta potential was again slightly less negative relative to citrate-stabilized 40-nm AgNPs (**Figure S6c,d**). The adsorption of GaHb on AgNPs can be expected to displace surface-bound citrate and produce a less negative zeta potential, as its own zeta potential is also modestly negative (–10 mV).

Table S1. Mean hydrodynamic sizes and zeta potentials of AgNPs and GaHb–AgNPs

Sample ^a	Zeta Potential (mV) ^b	Mean d_h (nm) ^b
10-nm AgNP	–34.4	14
10-nm GaHb–AgNP	–19.0	17
40-nm AgNP	–31.9	36
40-nm GaHb–AgNP	–27.5	34

^a Initial sizes provided by supplier. ^b Measured in 15 mM borate buffer (pH 8.5).

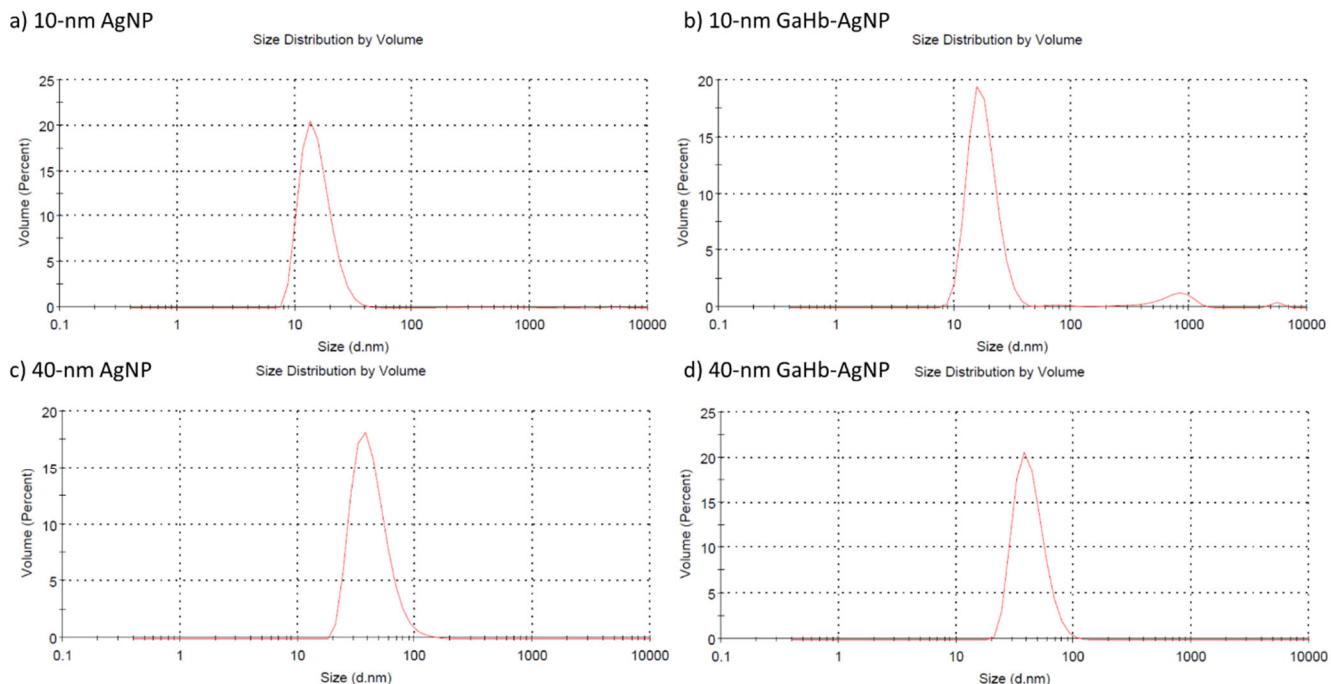


Figure S5. DLS size distribution peaks (number-based analysis) for (a) 10-nm AgNPs, (b) 10-nm GaHb–AgNPs, (c) 40-nm AgNPs, and (d) 40-nm GaHb–AgNPs.

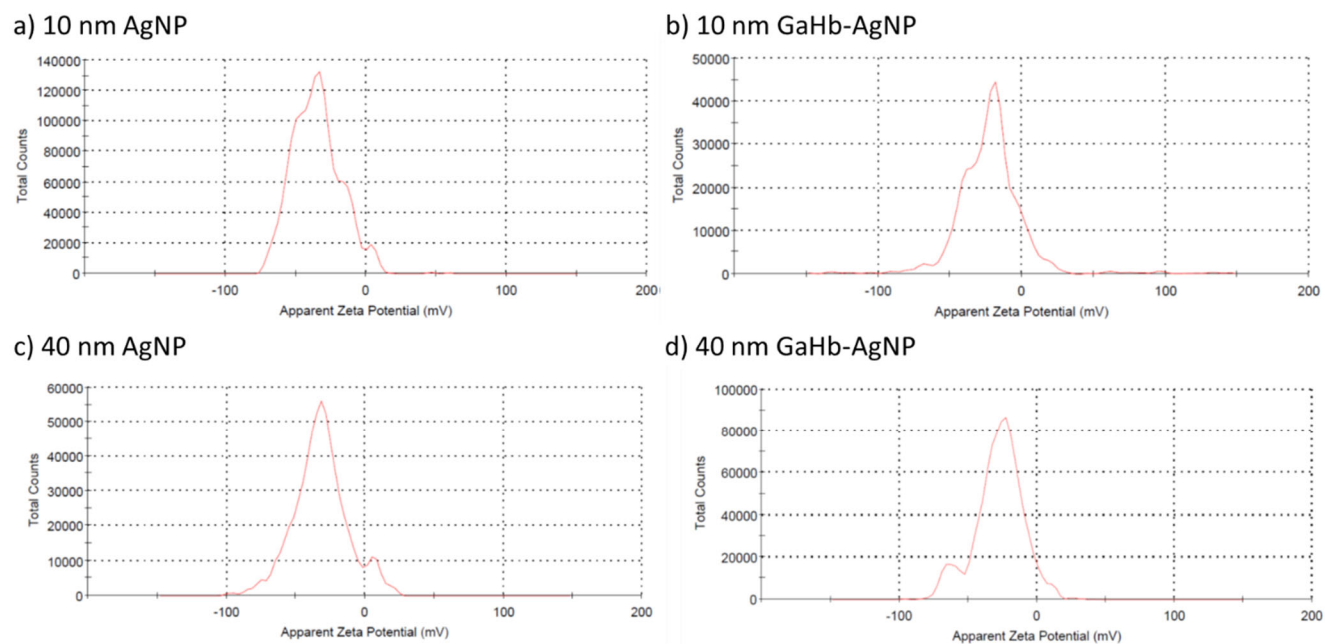


Figure S6. Zeta potentials for (a) 10-nm AgNPs, (b) 10-nm GaHb–AgNPs, (c) 40-nm AgNPs, and (d) 40-nm GaHb–AgNPs. All particles were dispersed in 15 mM borate buffer (pH 8.5).

Preparation and characterization of GaHb–AuNPs

Citrate-stabilized 10-nm Au nanoparticles were obtained as 50 $\mu\text{g}/\text{mL}$ solutions from a commercial source (NanoComposix). GaHb–AuNPs were prepared in a manner analogous to that of 10-nm GaHb–AgNPs; the mixture was slowly stirred overnight at 4 $^{\circ}\text{C}$, then transferred to a centrifugal filter tube (Centricon, 100-kDa MWCO) and subjected to 2700 g for 5 min, followed by dilution of the residual suspension in 15 mM borate buffer (pH 8.5). A Bradford assay yielded a weight ratio of 1 μg of GaHb per 11.4 μg of Au, corresponding to 8 GaHb per AuNP.

Absorbance spectroscopy of GaHb–AuNPs indicated a peak at 529 nm, a 9-nm redshift in plasmon resonance of the AuNP core relative to citrate-stabilized (uncoated) AuNPs (**Figure S7a**). The mean h_d was evaluated by DLS and found to be 25 nm, whereas that of uncoated AuNPs was 14 nm (**Figure S7b,c**).

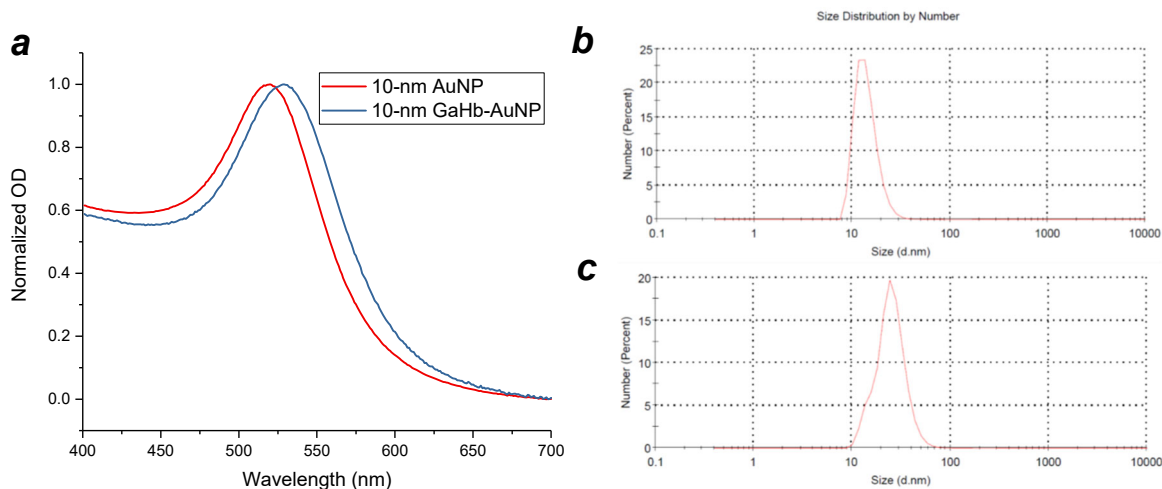


Figure S7. (a) Absorbance spectra of citrate-stabilized AuNPs and 10-nm GaHb–AuNPs dispersed in borate buffer; (b) DLS analysis for (b) 10-nm AuNPs and (c) 10-nm GaHb–AuNPs.

Cytotoxicity studies of GaHb–AgNPs using HaCaT and J774 cells

The cytotoxicity of 10-nm GaHb–AgNPs against keratinocytes was evaluated by measuring mitochondrial activity following exposure (MTT assay). HaCaT cells (AddexBio) were cultured in Dulbecco's Modified Eagle Medium (DMEM) containing 10% FBS at 37 $^{\circ}\text{C}$ in a 5% CO_2 atmosphere with multiple passages before use. Approximately 10^6 HaCaT cells were plated in a T-25 flask and grown to 70–80% confluence in 5 mL of medium over a period of 1 day. The adherent cells were washed with PBS, then released into media by treatment with 0.25% trypsin/EDTA at room temperature and counted using a haemocytometer. A 0.8-mL suspension containing 10^6 cells was diluted with 7.2 mL of growth

medium and added to a 96-well plate in 80- μ L aliquots (10^4 cells/well), then incubated for 18–24 hours at 37 °C. Experimental wells were treated with 20- μ L aliquots of 10-nm GaHb–AgNP (40–200 μ g/mL), with final concentrations ranging from 5.8 to 46 μ g/mL, then incubated for an additional 22 hours in the dark at 37 °C. Control wells were treated with 20 μ L of 0.005% Triton X-100 in growth medium (TX-100; Ctrl⁺) or medium alone (Ctrl⁻). All experiments were performed in triplicate.

Cell viability assays were performed by adding 10 μ L of MTT reagent (5 mg/mL) to each well then incubating for 4 hours at 37 °C, followed by addition of 100 μ L of detergent (10% Triton X-100 + 0.1 M HCl in isopropanol) to halt MTT oxidation and fix the cells. Plates were covered with aluminum foil and left on a shaker overnight at room temperature, then read at 570 nm (main absorbance) and 650 nm (background). No appreciable dark toxicity was observed at any concentrations (**Figure S8a**). Instead, GaHb–AgNP treatment resulted in significant increases in activity, which we postulate to be a hormetic response to non-lethal ROS levels.

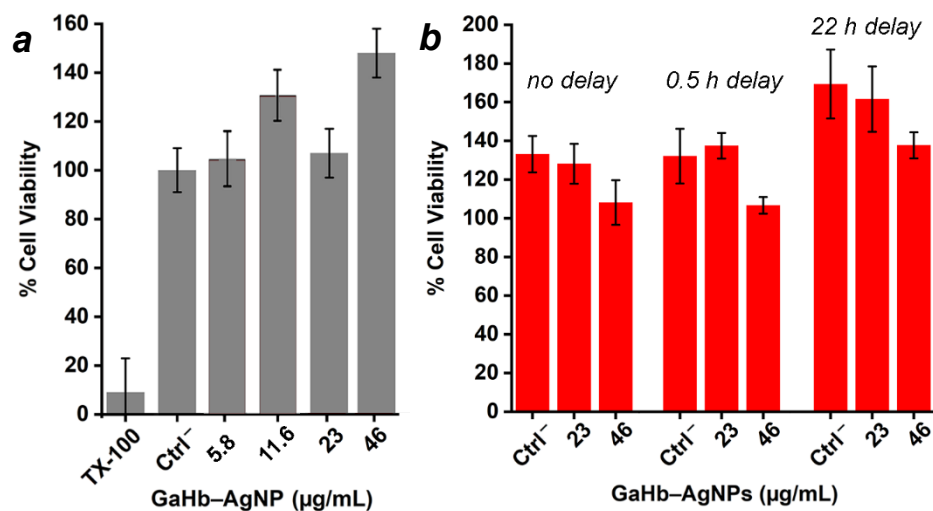


Figure S8. (a) Cytotoxicity studies of 10-nm GaHb–AgNPs against HaCaT cells; Controls include cells without GaHb–AgNPs (Ctrl⁻) or treated with Triton X-100 (TX-100).

(b) Phototoxicity studies of GaHb–AgNPs against HaCaT cells, with a 10-s exposure to 405-nm LED source (1.4 J/cm^2) after variable delay periods. The increased activity in the 22-h delay is likely due to longer overall incubation time.

Phototoxicity studies were performed by incubating HaCaT cells with GaHb–AgNPs (23 or 46 μ g/mL) at 37 °C at three different time intervals (0, 0.5, or 24 hours) to address NP uptake as a variable, then irradiated with a 405-nm LED array for 10 seconds at 140 mW/cm^2 . Cells were incubated for an additional 22 hours in the dark at 37 °C, then evaluated by MTT assay (**Figure S8b**). Some phototoxicity was observed for cells with the highest GaHb–AgNP concentration (46 μ g/mL), although this appears to be compensated by light-stimulated mitochondrial activity.

Similar studies were performed using J774 macrophages. Unlike keratinocytes, irradiation of J774 cells with 405-nm light did not stimulate any significant growth or mitochondrial activity. GaHb–AgNPs had negligible dark toxicity against J774 cells except at the highest concentration (46 $\mu\text{g/mL}$), but significant cytotoxicity was observed if irradiated by the 405-nm LED source immediately after treatment (**Figure S9**). Introducing a 24-hour delay between GaHb–AgNP addition and 405-nm irradiation reduced phototoxicity to low levels, indicating the sequestration or degradation of photoactive agent.

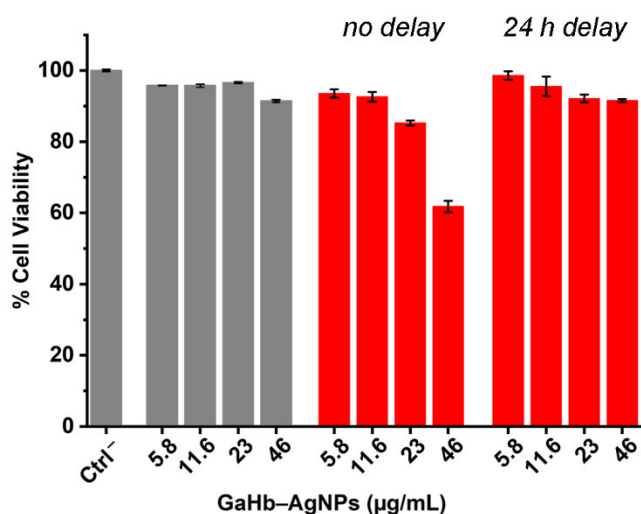


Figure S9. (a) Cytotoxicity studies of 10-nm GaHb–AgNPs against J774 cells, in the dark and after 10-s exposure to 405-nm irradiation (1.4 J/cm^2). Cells without GaHb–AgNPs were included as a control (Ctrl-).

Additional TEM images of *S. aureus* labeled with 10-nm GaHb–AgNPs

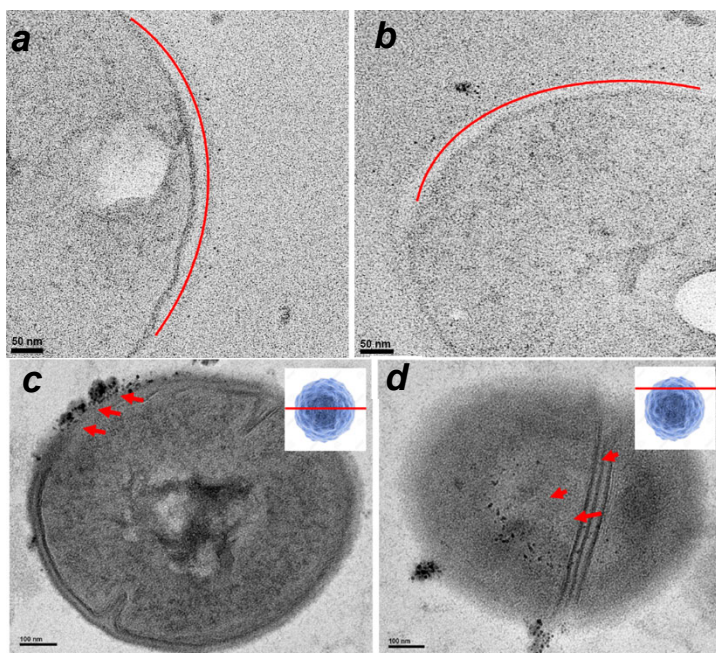


Figure S10. (a,b) TEM images (Tecnai T20, 200 kV) of GaHb–AgNP labeled bacteria without staining or sectioning by microtomy, showing random distribution along cell wall (demarcated by red trace). (c,d) TEM images of GaHb–AgNP labeled bacterium sectioned by microtomy. (c) Central section with GaHb–AgNP along outer wall (same as Figure 10); (d) polar “cap” decorated with GaHb–AgNP.

Studies involving MRSA persister cells and intracellular MRSA

To generate persister cells, MRSA was treated with ciprofloxacin as described elsewhere.²⁸ Briefly, a logarithmic culture of MRSA USA300 in tryptic soy (TS) broth was exposed to $10 \times$ MIC ciprofloxacin for 6 hours. The surviving bacteria were then treated with GaHb–AgNPs, irradiated for 10 seconds with 405-nm light, and incubated at 37 °C. Aliquots were withdrawn following light irradiation, diluted, and counted to determine CFU/mL. Controls included broth alone and addition of GaHb–AgNPs without light.

To generate intracellular bacteria, murine macrophage cells (J774) were infected with MRSA as described elsewhere.²⁹ J774 cells were first cultured in DMEM supplemented with 10% FBS at 37 °C with 5% CO₂, then exposed to MRSA USA400 at a multiplicity of infection of approximately 10:1. Host cells were washed 1-h post-infection with gentamicin (200 µg/mL) to kill extracellular MRSA. GaHb–AgNPs in buffer was added at several different concentrations with 10-s exposure to 405-nm light or kept in the dark, then incubated for 24 hours. J774 cells were treated again with gentamicin (50 µg/mL) and subsequently lysed using 0.1% Triton-X 100. The solution was serially diluted in PBS and transferred to TS agar plates in order to determine viable MRSA within the J774 cells. Plates were incubated at 37 °C for 18–22 hours before counting viable colonies.

Light sources for antimicrobial photodynamic inactivation

Light sources for this study include a custom-built, 405-nm LED array (Rainbow Technology Systems, Glasgow, UK) with a net radiant flux rated at 3 W/in² (465 mW/cm²), and a 20-W compact fluorescent lightbulb (CFL; Sunlite SL20/BLB) housed in an ellipsoidal reflector dome. The LEDs are monochromatic with similar spacings as those used in 96-well microtiter plates, corresponding to one LED per well. The irradiance of individual LEDs at maximum power was measured in the UV/V spectral region using a UV PowerMAP (EIT, Leesburg, VA) positioned 8 mm away, with peak power densities of 140 mW/cm². The CFL produces three emission bands as measured using an Acton SpectraPro 2300i spectrometer (Princeton Instruments, Acton, MA; 1200 gratings/inch), with two major peaks at 406 and 438 nm and a third minor peak at 548 nm. Irradiance from the CFL source was measured with a handheld luminometer (Lux/FC HS1010A) and a 425-nm shortpass filter positioned 4 cm away, yielding 31 lux or a mean power density of 12.4 mW/cm² for emission at 406 nm. Both light sources generate minor increases in surface temperature, with 10-s irradiation by the LED source producing less than a 3 °C increase and 15-min irradiation by the CFL source producing a 5 °C increase. More details on the LED array and emission spectrum of the CFL source at DOI: 10.1021/acsinfecdis.8b00125.¹³